

Plasmonic coupling of silver nanoparticles covered by hydrogen-terminated graphene for surface-enhanced Raman spectroscopy

Chih-Yi Liu,^{1,2} Keng-Chih Liang,^{1,2} Waileong Chen,³ Chia-hao Tu,⁴ Chuan-Pu Liu,⁴ and Yonhua Tzeng^{1,3,*}

¹Advanced Optoelectronic Technology Center, National Cheng Kung University, No.1, University Road, Tainan 701, Taiwan

²Department of Photonics, National Cheng Kung University, No.1, University Road, Tainan 701, Taiwan

³Institute of Microelectronics, National Cheng Kung University, No. 1, University Road, Tainan 701, Taiwan

⁴Department of Materials Science and Engineering, National Cheng Kung University, No. 1, University Road, Tainan 701, Taiwan

*tzengyo@mail.ncku.edu.tw

Abstract: We report on strong plasmonic coupling from silver nanoparticles covered by hydrogen-terminated chemically vapor deposited single-layer graphene, and its effects on the detection and identification of adenine molecules through surface-enhanced Raman spectroscopy (SERS). The high resistivity of the graphene after subjecting to remote plasma hydrogenation allows plasmonic coupling induced strong local electromagnetic fields among the silver nanoparticles to penetrate the graphene, and thus enhances the SERS efficiency of adenine molecules adsorbed on the film. The graphene layer protects the nanoparticles from reactive and harsh environments and provides a chemically inert and biocompatible carbon surface for SERS applications.

©2011 Optical Society of America

OCIS codes: (220.4241) Nanostructure fabrication; (230.0250) Optoelectronics; (240.6680) Surface plasmons; (250.5403) Plasmonics; (310.6628) Subwavelength structures, nanostructures; (240.0240) Optics at surfaces; (240.6695) Surface-enhanced Raman scattering.

References and links

1. S. E. J. Bell and N. M. S. Sirimuthu, "Surface-enhanced Raman spectroscopy (SERS) for sub-micromolar detection of DNA/RNA mononucleotides," *J. Am. Chem. Soc.* **128**(49), 15580–15581 (2006).
2. F. Ortmann, W. G. Schmidt, and F. Bechstedt, "Attracted by long-range electron correlation: adenine on graphite," *Phys. Rev. Lett.* **95**(18), 186101 (2005).
3. H. H. Wang, C. Y. Liu, S. B. Wu, N. W. Liu, C. Y. Peng, T. H. Chan, C. F. Hsu, J. K. Wang, and Y. L. Wang, "Highly Raman-enhancing substrates based on silver nanoparticle arrays with tunable sub-10 nm gaps," *Adv. Mater. (Deerfield Beach Fla.)* **18**(4), 491–495 (2006).
4. T. T. Liu, Y. H. Lin, C. S. Hung, T. J. Liu, Y. Chen, Y. C. Huang, T. H. Tsai, H. H. Wang, D. W. Wang, J. K. Wang, Y. L. Wang, and C. H. Lin, "A high speed detection platform based on surface-enhanced Raman scattering for monitoring antibiotic-induced chemical changes in bacteria cell wall," *PLoS ONE* **4**(5), e5470 (2009).
5. C.-H. Huang, H.-Y. Lin, B.-C. Lau, C.-Y. Liu, H.-C. Chui, and Y. Tzeng, "Plasmon-induced optical switching of electrical conductivity in porous anodic aluminum oxide films encapsulated with silver nanoparticle arrays," *Opt. Express* **18**(26), 27891–27899 (2010).
6. T. Atay, J.-H. Song, and A. V. Nurmikko, "Strongly interacting plasmon nanoparticle pairs: from dipole–dipole interaction to conductively coupled regime," *Nano Lett.* **4**(9), 1627–1631 (2004).
7. C. H. Huang, H. Y. Lin, C. H. Lin, H. C. Chui, Y. C. Lan, and S. W. Chu, "The phase-response effect of size-dependent optical enhancement in a single nanoparticle," *Opt. Express* **16**(13), 9580–9586 (2008).
8. C. H. Huang, H.-Y. Lin, S. Chen, C.-Y. Liu, H.-C. Chui, and Y. Tzeng, "Electrochemically fabricated self-aligned 2-D silver/alumina arrays as reliable SERS sensors," *Opt. Express* **19**(12), 11441–11450 (2011).
9. C. Y. Liu, M. M. Dvoynenko, M. Y. Lai, T. H. Chan, Y. R. Lee, J.-K. Wang, and Y. L. Wang, "Anomalously enhanced Raman scattering from longitudinal optical phonons on Ag-nanoparticle-covered GaN and ZnO," *Appl. Phys. Lett.* **96**(3), 033109 (2010).
10. L. Xie, X. Ling, Y. Fang, J. Zhang, and Z. Liu, "Graphene as a substrate to suppress fluorescence in resonance Raman spectroscopy," *J. Am. Chem. Soc.* **131**(29), 9890–9891 (2009).

11. X. Ling, L. Xie, Y. Fang, H. Xu, H. Zhang, J. Kong, M. S. Dresselhaus, J. Zhang, and Z. Liu, "Can graphene be used as a substrate for Raman enhancement?" *Nano Lett.* **10**(2), 553–561 (2010).
12. D. C. Elias, R. R. Nair, T. M. G. Mohiuddin, S. V. Morozov, P. Blake, M. P. Halsall, A. C. Ferrari, D. W. Boukhvalov, M. I. Katsnelson, A. K. Geim, and K. S. Novoselov, "Control of graphene's properties by reversible hydrogenation: evidence for graphane," *Science* **323**(5914), 610–613 (2009).
13. A. Gupta, G. Chen, P. Joshi, S. Tadigadapa, and P. C. Eklund, "Raman scattering from high-frequency phonons in supported n-graphene layer films," *Nano Lett.* **6**(12), 2667–2673 (2006).
14. M. E. Kompan and D. S. Krylov, "Detecting graphene-graphane reconstruction in hydrogenated nanoporous carbon by Raman spectroscopy," *Tech. Phys. Lett.* **36**(12), 1140–1142 (2010).
15. C. Otto, T. J. J. van den Tweel, F. F. M. de Mul, and J. Greve, "Surface-enhanced Raman spectroscopy of DNA bases," *J. Raman Spectrosc.* **17**(3), 289–298 (1986).
16. H. Watanabe, Y. Ishida, N. Hayazawa, Y. Inouye, and S. Kawata, "Tip-enhanced near-field Raman analysis of tip-pressurized adenine molecule," *Phys. Rev. B* **69**(15), 155418 (2004).
17. N. Hayazawa, H. Watanabe, Y. Saito, and S. Kawata, "Towards atomic site-selective sensitivity in tip-enhanced Raman spectroscopy," *J. Chem. Phys.* **125**(24), 244706 (2006).
18. J. E. Freund, M. Edelwirth, P. Kröbel, and W. M. Heckl, "Structure determination of two-dimensional adenine crystals on graphite," *Phys. Rev. B* **55**(8), 5394–5397 (1997).
19. K. Berland, S. D. Chakarova-Käck, V. R. Cooper, D. C. Langreth, and E. Schröder, "A van der Waals density functional study of adenine on graphene: single-molecular adsorption and overlayer binding," *J. Phys. Condens. Matter* **23**(13), 135001 (2011).
20. Y. Tian and T. Tatsuma, "Mechanisms and applications of plasmon-induced charge separation at TiO₂ films loaded with gold nanoparticles," *J. Am. Chem. Soc.* **127**(20), 7632–7637 (2005).
21. H. Y. Lin, C. H. Huang, C. H. Chang, Y. C. Lan, and H. C. Chui, "Direct near-field optical imaging of plasmonic resonances in metal nanoparticle pairs," *Opt. Express* **18**(1), 165–172 (2010).
22. I. Romero, J. Aizpurua, G. W. Bryant, and F. J. García De Abajo, "Plasmons in nearly touching metallic nanoparticles: singular response in the limit of touching dimers," *Opt. Express* **14**(21), 9988–9999 (2006).
23. N. W. Liu, C. Y. Liu, H. H. Wang, C. F. Hsu, M. Y. Lai, T. H. Chuang, and Y. L. Wang, "Focused-ion-beam-based selective closing and opening of anodic alumina nanochannels for the growth of nanowire arrays comprising multiple elements," *Adv. Mater. (Deerfield Beach Fla.)* **20**(13), 2547–2551 (2008).
24. K. T. Tsai, Y. R. Huang, M. Y. Lai, C. Y. Liu, H. H. Wang, J. H. He, and Y. L. Wang, "Identical-length nanowire arrays in anodic alumina templates," *J. Nanosci. Nanotechnol.* **10**(12), 8293–8297 (2010).

1. Introduction

Surface-enhanced Raman spectroscopy (SERS) is a promising photonic technology for rapid detection and identification of biomedical molecules such as DNA [1,2]. When closely spaced noble metal nanoparticles are illuminated by light of a proper wavelength, surface plasmon resonance and plasmonic coupling among nanoparticles are induced [3–5]. The collective oscillation of surface plasmons results in significantly increased absorption/scattering cross-section of nanoparticles and an enhanced local electromagnetic field [6,7]. When molecules are present in the strong field, their Raman signals are greatly enhanced. Each kind of molecules has its unique SERS, which can be applied to detect and identify them. Although SERS is a powerful technique, reactions of metal nanoparticles with the target molecules and the environments often severely degrade its performance. Therefore, for applications where environmental compatibility, data repeatability, and measurement specificity are important, encapsulation of metal nanoparticles by a chemically inert thin film, through which, plasmonic coupling can penetrate easily, is desirable.

In a previous work [8], we have demonstrated the use of thin residual alumina barrier layer for encapsulating silver nanoparticles for SERS applications. It showed that the thinner the alumina barrier layer is, the better the SERS enhancement is. Strong local electromagnetic fields induced by plasmonic coupling on silver nanoparticles decay in intensity rapidly with an increasing distance from the nanoparticles. Therefore, when a protective dielectric film is coated on the nanoparticles, the thinner the film is, the better the strong electromagnetic fields can be applied to the molecules adsorbed on the surface of the dielectric film. Although alumina has been found to be an excellent protective dielectric, precise control of pin-hole free alumina thickness down to as thin as a single-layer graphene of one atom thick is not practical. It is, therefore, worthy the demonstration of the feasibility of applying the thinnest possible stable film of one atom thick, e.g., single-layer graphene as a protective film for silver nanoparticles based plasmonic devices. The optimization for the overall performance of graphene protected SERS devices is beyond the scope of this paper and is being undertaken to be reported in a separated paper.

It has been reported that graphene was used as a SERS substrate to help quench fluorescence and chemically enhance SERS scattering by charge transfer [9] from molecules to the graphene substrate [10,11]. The chemical SERS enhancing factor is many orders of magnitude lower than optimized SERS enhanced by plasmonic coupling induced electromagnetic field [11]. When a conductive thin film is applied to cover metal nanoparticles, the conductive thin film distorts the field distribution and suppresses the electromagnetic field lines near and parallel to the surface of the thin film where molecules to be detected are attached. A dielectric or high resistivity thin film is desirable. However, single-layer graphene is conductive. Fully hydrogenated single-layer graphene is known to become electrically insulating graphene [12]. In this work, silver nanoparticles are covered by hydrogen-terminated (H-terminated) single-layer graphene as SERS substrates for detecting adenine.

2. Experimental

A silver thin film with thickness of ~8 nm was deposited on a surface oxidized silicon wafer by thermal evaporation in high vacuum. Thermal annealing caused the silver film to form silver nanoparticles on the oxide surface. Single-layer graphene was synthesized on a copper foil by means of low-pressure thermal chemical vapor deposition (CVD) in a gas mixture of methane and hydrogen and then transferred to cover the Ag/silicon-dioxide/silicon substrate after the copper foil was removed by wet chemical etching. Raman spectroscopy reveals well-known D-peak, G-peak, and 2D-peak, with the intensity of the 2D-peak higher than that of the G-peak, characteristic of single-layer graphene [13]. Gold contact electrodes were deposited on two ends of the graphene sheets for resistance measurements. The underlying silver nanoparticles are of about 100 nm in size and inter-particle distance. Electrical resistance was measured between these two gold electrodes before and after hydrogenation.

Hydrogen termination of the graphene/Ag/silicon-dioxide/silicon substrate was carried out in a microwave plasma reactor where a plasma ball was generated by 200 W microwave of 2.45 GHz at 1 Torr hydrogen gas pressure. The graphene surface was at a distance of about 10 cm from the plasma ball with a metal screen in between. After each plasma treatment, electrical resistance was measured. The resistance as a function of the exposure time of the graphene to the remote hydrogen plasma is, thus, measured.

Adenine solutions of 10^{-4} to 10^{-7} M are used for SERS measurements. The solution was prepared by dissolving adenine powder in deionized water. Pristine and H-terminated substrates were dipped in the solution for 1 hour. Raman spectra were measured from the wet samples in air by a backward micro-Raman spectroscopy with an excitation light of 532 nm. Wet samples were chosen for measurements in preparation for future applications of SERS to biomedical sensing. All the Raman spectra were measured under the same conditions, such as laser power and detection time, for effective comparisons.

3. Results and discussion

Figure 1(a) shows an optical micrograph near the boundary between the pristine and H-terminated areas in a hydrogen plasma-treated graphene film (single atomic layer) on Ag nanoparticles. Half of the graphene was covered by a mask in order to hydrogenate only the other half of the graphene. The color difference between the two areas as shown in the optical micrograph allows selected areas for SERS measurements as a comparison. The boundary is shown by the SEM micrographs of Figs. 1(b) and 1(c). Higher electrical resistance of hydrogen-terminated single-layer graphene is shown to be brighter than the pristine one in SEM micrographs. Electron beam can easily penetrate through the atomically thin graphene layer to display underlying silver nanoparticles of about 100 nm in size, as shown in Fig. 1(c).

Figure 2(a) shows the electrical resistance of a graphene/Ag/silicon-dioxide/silicon substrate as a function of remote hydrogen plasma exposure time. In this work, electrical conduction between silver nanoparticles on silicon dioxide is negligible considering the large separation between silver nanoparticles of about 100 nm. Graphene is grown on copper foil, which is much more conductive than graphene. The resistance of the graphene before transfer

is not measured. The resistance of transferred graphene on silicon dioxide does not vary much whether there are underlying silver nanoparticles of the size and interspacing used in this work. Gold contact pads are deposited through a shadow mask on two sides of a rectangular graphene sheet transferred onto silver nanoparticles coated silicon dioxide surface. This leaves an exposed square graphene sheet of 1 cm on each side. The gold contact pads help protect the underlying graphene sheet from being hydrogenated and retain the contact resistance. The exact contact resistance is not measured; but, it is known to be lower than the measured much lower total resistance for the graphene before hydrogenation and two contact pads than the resistance of hydrogenated graphene. This allows the high resistance of the exposed and hydrogenated graphene to be measured. Since the exposed graphene sheet is of a square shape with each side being about 1 cm, the measured resistance of the graphene, after taking the contact resistance into account, is also an indication of the sheet resistance of the graphene. Therefore, the measured total resistance is appropriate to exhibit the effects of hydrogenation on the sheet resistance of the graphene, especially for hydrogenated graphene, to which the contribution by low contact resistance to the measured very high total resistance is small.

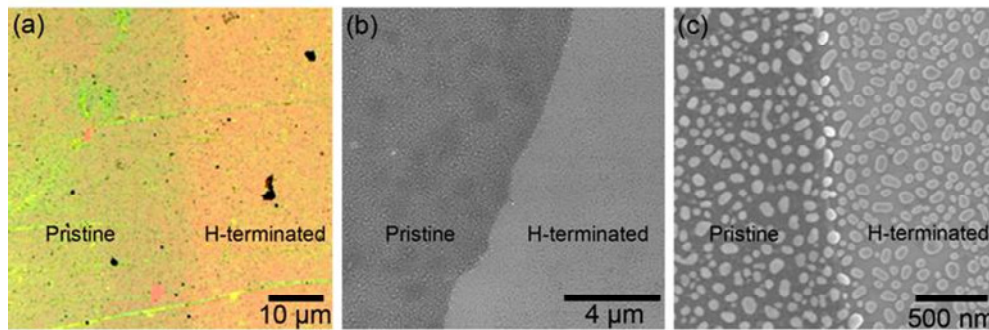


Fig. 1. (a) Optical, (b) large-scale and (c) small-scale SEM micrographs showing the boundaries between pristine and H-terminated graphenes covering silver nanoparticles. The shown H-terminated area has been subjected to the remote hydrogen plasma treatment for 65 minutes.

The measured resistance is dominated by the graphene film since Ag nanoparticles are well separated and the silicon dioxide is an insulator. It clearly shows that the resistance initially increases gradually with the exposure time and then the increase speeds up. For short exposure time, hydrogen is scarcely distributed on the graphene surface. Many conductive paths without hydrogen termination are still present. As a result, the increasing rate of resistance is low. As the exposure time increases further, a higher fraction of the graphene surface is terminated by hydrogen and the conductive path becomes scarce leading to rapid increase in electrical resistance. When the entire surfaces are terminated by hydrogen, the graphene is expected to become insulating and known as graphane. For the following work, single-layer graphene after exposure to remote hydrogen plasma for 65 minutes is used for SERS measurements. As shown in Fig. 2(a), the treatment leads to a resistance of 200 k Ω , which is about 100 times larger than that of the graphene sheet before hydrogenation.

Figure 2(b) displays Raman spectra excited by 532-nm light for pristine graphene and H-terminated graphene with a spectrum for silicon-dioxide/silicon as a reference. Characteristic graphene peaks such as the D-peak (1328 cm^{-1}) and G-peak (1577 cm^{-1}) are shown in the spectra for pristine graphene and H-terminated graphene, but not in that for the silicon-dioxide/silicon substrate. The G-peak corresponds to optical E_{2g} phonons at the Brillouin zone center. The D-peak is caused by breathing-like modes corresponding to transverse optical phonons near the K point and requires a defect for its activation via an intervalley double-resonance Raman process. It is a measure of the amount of disorder including those of the domain boundaries in the graphene sheet. The 2D-peak, an overtone of the D-peak, is the sum of two phonons with opposite momentum and, therefore, exhibits a high intensity even

without defects. It reflects the electronic structure of the graphene with an increasing number of layers in the form of changes in the shape, width, and position of the peak via a double resonant Raman process. The 2D-peak is symmetric with the peak height being greater than that of the G-peak and the ratio of the integrated area under it to that for the G-peak being greater than 2, indicating that it is a single-layer graphene.

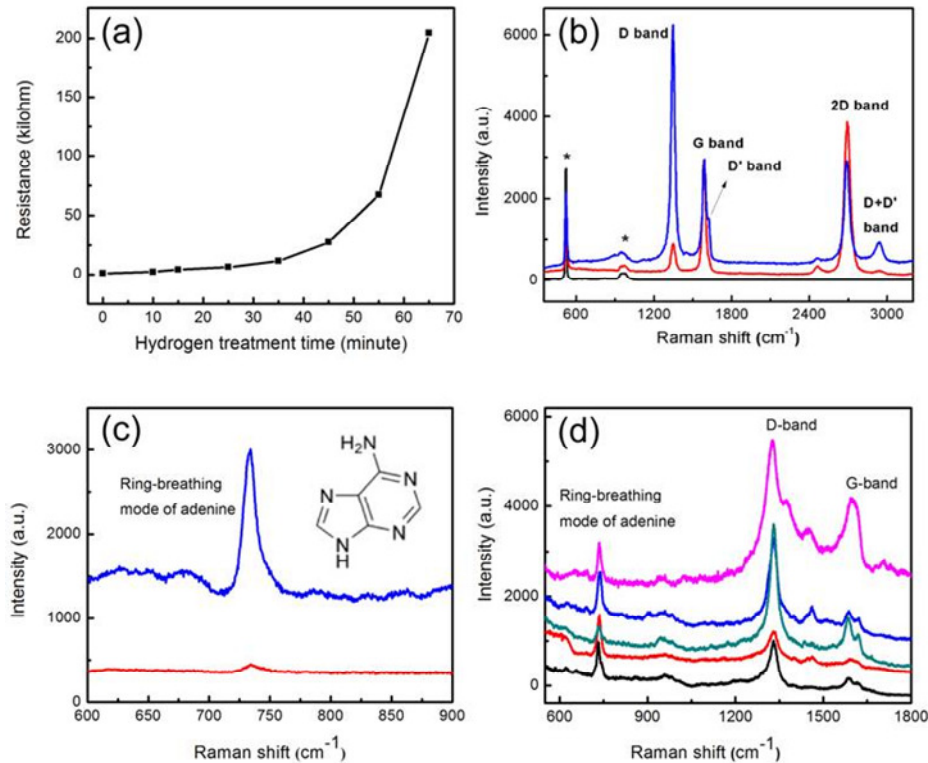


Fig. 2. (a) Electrical resistance of a graphene/Ag/silicon-dioxide/silicon substrate after exposure to remote plasma in hydrogen for up to 65 minutes. Resistance is measured between two gold contacts on two sides of a rectangular graphene sheet with a 1cm x 1cm exposed graphene. (b) Typical Raman spectra of a substrate before (middle red) and after (top blue) plasma treatment. The black curve (bottom) shows the Raman spectrum from a silicon dioxide/Si substrate. The star marks indicate the peaks from silicon-dioxide/silicon substrate. (c) SERS spectra of adenine molecules displaying the ring-breathing mode of adenine on H-terminated (top blue) and pristine (bottom red) substrates. (d) SERS spectra of adenine molecules measured in five different areas on a H-terminated substrate. The plasma treatment time period is 65 minutes for (b), (c), and (d). The inset in (c) schematically depicts molecular structure of adenine. The spectra are shifted vertically by different degrees for clearance.

Hydrogenated graphene exhibits slightly broadened 2D-peak and G-peak, both with decreased intensities relative to the D-peak. The intensity of the D-peak increases significantly after hydrogenation and is attributed to the breaking of the translational symmetry of sp^2 C-C bonds by atomic hydrogen. This also causes the G-peak intensity to decrease. The modified electronic structure of graphene by atomic hydrogen leads to the decrease in the 2D-peak as well. Hydrogenation of graphene also results in the appearance of the D' -peak on the shoulder of the G-peak. It occurs via an intravalley double-resonance process in the presence of defects. A combination mode, called D + D'-peak, of low intensity also appears on the high wavenumber side of the 2D-peak due to the combination of two phonons with different momentum and requires a defect for its activation [14].

Hydrogen-terminated graphene and pristine graphene on Ag/silicon-dioxide/silicon architectures were used as SERS substrates to examine adenine molecules, as shown in Fig.

2(c). A prominent peak of 732 cm^{-1} , originating from ring-breathing mode of adenine [15–17], is displayed in both spectra. Other less intensive peaks of adenine are hardly detected. This is attributed to the geometry of adsorption by adenine molecules on the SERS substrate. It has been reported that according to calculation, when an adenine molecule is adsorbed on graphene or graphite, the adenine atomic ring tends to adhere to the substrate surface to form a small angle with respect to the surface. The adenine atomic ring is, therefore, nearly parallel to the substrate surface and is the major excitation mode by the strong local electromagnetic fields induced on the SERS substrate by laser excitation of underlying silver nanoparticles [18,19]. As a result, the ring-breathing mode Raman signal of adenine is clearly displayed in Fig. 2(c).

Although both spectra in Fig. 2(c) show the signals of the ring-breathing mode, the peak intensity for H-terminated graphene is much higher than that for the pristine graphene. This is believed to originate from the difference in electrical conductivity of these two kinds of graphene layers which cover silver nanoparticles. For the pristine-graphene covered SERS substrate, local electric fields on and parallel to the graphene surface are to some extent short-circuited by the conductive graphene surface. Therefore, adenine atomic rings attached to the SERS substrate at a small angle is not subjected to the excitation by strong plasmonic coupled local electromagnetic fields. For the H-terminated SERS substrate, the high resistance hydrogenated graphene behaves more like the alumina dielectric layer covering silver nanoparticles in reference [8] Local strong electric fields in directions parallel to and on the graphene surface are allowed. Surface adsorbed adenine rings are preferentially excited by the strong plasmonic coupled local fields on the surface of the SERS substrate to produce a strong Raman signal.

Besides the effects of electromagnetic enhancement and suppression of surface fields by conductive graphene, the extent of the effects of adenine adsorption density on pristine graphene as compared to that on hydrogenated graphene are not clear. There are no reports on the adsorption power of adenine molecule on H-terminated graphene. However, it has been reported that adenine molecules could effectively adsorb on graphene [19]. Therefore, we believe that the electromagnetic enhancement is predominantly responsible for the high SERS signal intensity for adenine adsorbed on hydrogenated graphene with underlying silver nanoparticles. In brief, the measured spectra shown in Fig. 2(c) have clearly demonstrated that H-terminated single-layer graphene is a better film for covering silver nanoparticles as a SERS substrate than pristine single-layer graphene for the detection of adenine.

Figure 2(d) shows SERS spectra measured in five arbitrarily selected areas on an H-terminated graphene covered SERS substrate with adsorbed adenine molecules. All spectra display clear ring-breathing-peak of adenine along with the G-peak and D-peak of H-terminated graphene. Some detailed discrepancies are observed between spectra due to the non-uniform distributions of adenine, Ag dispersion, hydrogen termination, or graphene defects. Nevertheless, clear adenine peak of 732 cm^{-1} implies that the entire SERS substrate can be used for SERS detection of adenine.

To examine if the SERS substrate made of H-terminated graphene covered silver nanoparticles is reusable for SERS measurements, a SERS substrate is soaked in 10^{-4} M adenine solution, then cleaned by 10% alcohol, and finally re-soaked in the same solution again. After each of the three steps, Raman spectrum, as shown in Fig. 3(a), was measured. The ring-breathing peak of adenine appears after step 1 and step 3. No signal was detected after step 2 which cleaned the surface of the SERS substrate and removed the previously adsorbed adenine. It indicates that adsorbed adenine molecules are effectively removed by the cleaning process and the SERS substrate is reusable.

The sensitivity of H-terminated SERS substrates was studied by soaking them in adenine solutions of different concentrations and then measuring the corresponding Raman spectra, as shown in Fig. 3(b). With increased adenine concentration, the adenine signal of ring-breathing

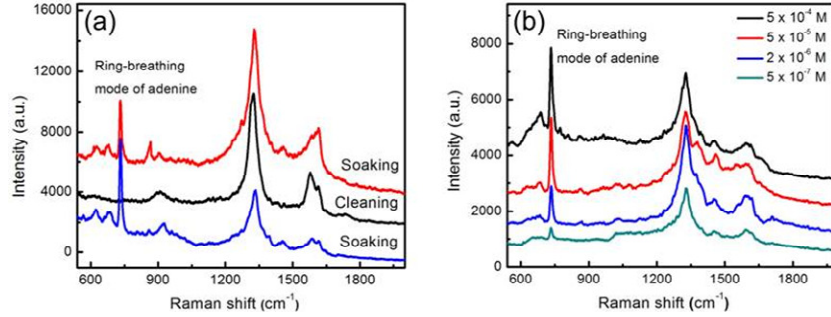


Fig. 3. (a) SERS spectra from an H-terminated substrate that was soaked in 10^{-4} M adenine (blue), then cleaned by 10% alcohol (black) and finally re-soaked in the solution (red). (b) SERS spectra corresponding to H-terminated substrates soaked in solutions with different adenine concentrations. The spectra are shifted vertically with different degrees for clearance.

mode became stronger. The figure indicates that the SERS substrate can be employed to detect adenine of concentration from 5×10^{-4} to 5×10^{-7} M. This work was aimed at studying the effectiveness of high-resistance hydrogen-terminated single-layer graphene to serve as an ultra-thin protective film for covering silver nanoparticles as SERS substrates. Further work is being undertaken to optimize the graphene synthesis, the hydrogenation process, and the underlying silver nanoparticles for high performance SERS applications [20–24].

4. Conclusions

Single-layer graphene terminated by hydrogen exhibits higher electrical resistivity and demonstrates superior SERS effects originating from underlying silver nanoparticles than pristine single-layer graphene. H-terminated graphene can be applied effectively as an atomically thin encapsulation layer for isolating molecules to be examined by SERS from the silver nanoparticles. With the silver nanoparticles being isolated from the molecules and environments of examination, the H-termination based SERS substrate is expected to enable many highly demanding applications such as biocompatible health care and medical research.

Acknowledgments

This work was partially supported by the Advanced Optoelectronic Technology Center, National Cheng Kung University, under projects from the Ministry of Education and National Science Council in Taiwan via grants 99-2120-M-006-004, 99-2911-I-006-504, 100-2221-E-006-169-MY3, and 100-2120-M-006-001.